Bull. Mater. Sci. (2019) 42:53
https://doi.org/10.1007/s12034-018-1715-y

Study on wear and corrosion properties of functionally graded nickel–cobalt–(Al_2O_3) coatings produced by pulse electrodeposition

A KARIMZADEH, M ALIOFKHAZRAEI* and A S ROUHAGHDAM
Department of Materials Engineering, Faculty of Engineering, Tarbiat Modares University, Tehran 1411713116, Iran
*Author for correspondence (maliofkh@gmail.com; khazraei@modares.ac.ir)

MS received 3 May 2017; accepted 27 July 2018; published online 21 February 2019

Abstract. Functionally graded nickel–cobalt coatings with/without alumina nanoparticles were pulse electrodeposited on a carbon steel substrate by a continuous decrease in duty cycle from 95 to 10% at different frequencies of 100, 500 and 1000 Hz. The effect of pulse parameters on the nanoparticle content, chemical composition, microstructure, corrosion properties and tribological behaviour of coatings was studied. Energy-dispersive X-ray spectroscopy analysis showed that the amount of cobalt is gradually reduced and the content of alumina nanoparticles is increased from the substrate/coating interface to the surface. Based on the electrochemical studies in 3.5 wt% NaCl, the nanocomposite coatings gain the highest corrosion resistance at the lowest frequency. Also, the hardness of coatings gradually increased. Evaluation of the tribological behaviour of coatings by a pin-on-disk wear test showed that the nanoparticles have a positive effect on wear resistance and improve it by increasing frequency.

Keywords. Nickel–cobalt; nanoparticles; gradient coatings; corrosion; wear.

1. Introduction

Nickel–cobalt alloys have been used as an important material in different industries for various reasons, such as high strength, high hardness, good wear resistance, good corrosion resistance, thermal conductivity, electrocatalytic properties, magnetic properties and even memory properties [1–6]. Co–Ni alloys have a high value of practical importance due to protective and decorative values. Among the methods of Ni–Co coating production, electrodeposition is largely used. This is because of its low cost, flexibility (single layer or multilayer deposition as intermittent or gradient), high efficiency and simple mass production procedure with no need for high temperatures and high pressures in comparison with other production methods such as sputtering and chemical vapour deposition [7–9]. Various studies have shown that the electrolytic deposition of Ni–Co alloys on carbon steel improves some properties such as hardness [10], wear resistance [11] and other mechanical properties [12] as well as corrosion resistance [13] in corrosive and abrasive environments in the presence of ceramic particle additives [14,15]. In fact, the electrochemical deposition of nanoparticles in the metallic matrix leads to combination of properties which cannot be achieved independently by the other metallurgical methods [16–18]. Uniform distribution of the nanoparticles, such as alumina, SiC, diamond, TiO_2, WC, etc. [18–21] can improve microhardness, wear resistance, corrosion resistance, high-temperature inertness and anti-oxidation coating properties [15,18].

One of the most important features of Ni–Co coatings is the possibility of compounds formation in approximately all chemical compounds as long as both Ni and Co are in the concentration range of a solid solution [22,23]. In fact, this feature leads to the formation of different coatings with various properties in different ranges of chemical compositions [24,25]. Composite coatings have been used extensively in various industries due to the improved properties, such as good adhesion, lower internal stress, higher hardness, good wear and corrosion resistance [18–20]. But some researchers [26–28] have shown that adhesion of the coating to the substrate is reduced by adding ceramic particles to the coating. Thereby, reducing the coating adhesion to the substrate results drop in some properties such as wear resistance [29,30]. To prevent this, researchers have suggested a functionally graded nanocomposite coating [30–32]. In fact, this coating is one of the functionally graded materials (FGM) with the concentration gradient of the alloy composition and the strengthener ceramic particles. The characteristic of the gradient material is that the properties change by variation of the composition and structure which show nanoparticles content changes steeply from the substrate to the coating surface and it, in fact, prevents from separation and poor adhesion of the coatings [30]. The amount of nanoparticles can be altered by various methods, such as electrodeposition parameters (for example, current density [30], stirring rate [33] and injection of nanoparticles into the solution [34] as well as changing the pulse parameters [35,36], such as frequency and duty cycle). An example of the electrodeposited gradient coatings created

by changing various electroplating parameters, includes Ni–(Al_2O_3) [37], Ni–Fe–(Al_2O_3) [38], Ni–W–(Al_2O_3) [39] and Ni–Co–SiC [40]. One of the advantages of functionally graded nanocomposite coating is the prevention of some mechanical properties dropping like decreasing the ductility due to the difference in mechanical properties between the hard particles and the soft substrate [41,42]. In fact, the value of mismatching at the coating/substrate interface is reduced and less stress is created at the interface due to the gradual change in the amount of nanoparticles [26]. Furthermore, the gradient structure alters the grain size and its plastic behaviour. Thus, propagation of the crack happens at the slower rate by changing the toughness of the crack tip [43]. Mechanical and corrosion property improvements have been observed in functionally graded nanocomposite coatings [30,44].

The aim of the present study is to develop Ni–Co and Ni–Co–(Al_2O_3) functionally graded coatings using the pulsed-electrodeposition method to change the amount of Ni, Co and alumina nanoparticles in a gradual manner. To achieve this purpose, a continuous change in pulse parameters (such as duty cycle) was applied in six stages and three different frequencies. Finally, microstructure, hardness, corrosion and wear properties of the coatings were studied and compared with each other.

2. Materials and methods

Low carbon steel sheets with dimensions of $1 \times 2 \times 5\,mm^3$ were used as substrates. Prior to the deposition process, the samples were polished to 1000 sanding grade. Then, the samples were washed with distilled water and degreased with acetone. Finally, the acid washing and activation of the samples were carried out in 10% hydrochloric acid for 10 s. The electrodeposition process was conducted in a 200 ml beaker using consumable pure nickel anodes. The coating was produced using the pulse-electrodeposition method. During the plating, pulse parameters were changed by using a pulse generator connected to a rectifier. Figure 1 shows the schematic of functionally graded coatings and the deposition process. The pulse generator automatically and continuously changes the pulse parameters (duty cycle) during the electrodeposition process. The coatings have been developed by making a continuous change in the duty cycle (by reducing it from the interface of coating/substrate to the coating surface).

Ni–Co and Ni–Co–(Al_2O_3) coatings were electrodeposited from a modified Watts bath containing cobalt sulphate (table 1). During the electrodeposition, the solution temperature was maintained at 50°C and pH was adjusted to 3.5 ± 0.5 using $NH_3 \cdot H_2O$ (10 wt%) and sulphuric acid (10%) solutions.

A transmission electron microscope image of alumina nanoparticles is shown in figure 2. The size of used alumina particles was in the range of 20 ± 5 nm. Alumina nanoparticles using magnetic stirring at 400 rpm were agitated for 12 h before starting the electrodeposition process. Then, the suspension was stirred using ultrasonic homogenizer instrument before electrodeposition. The ultrasonic agitation was performed at the power of 200 watts and 20 kHz frequency for 30 min.

The microstructure of the coatings was evaluated by scanning electron microscopy (SEM). In addition, the chemical analysis of coating layers was carried out using energy-dispersive X-ray spectroscopy analysis (EDS). Electrochemical measurements were conducted using an EG&G273A

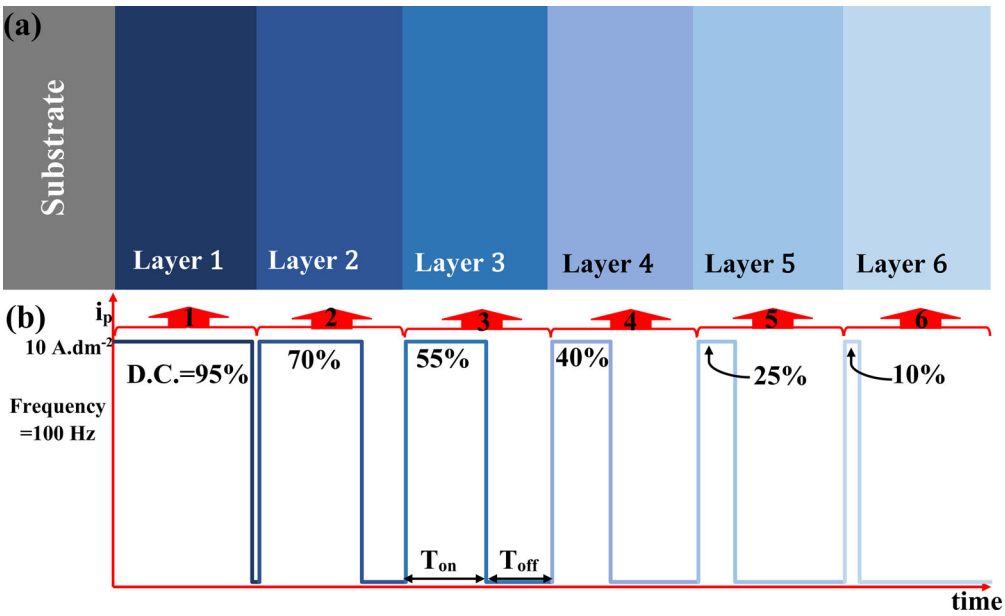

Figure 1. Schematic of (**a**) Ni–Co-(Al_2O_3) functionally graded coatings and (**b**) pulse current applied continuously by using a pulse generator during the electrodeposition process.

Table 1. Composition of an electrodeposition bath.

Parameter	Quantity (g l^{-1})
$NiSO_2{\cdot}6H_2O$	250
$NiCl_2{\cdot}6H_2O$	40
H_3BO_3	35
$CoSO_4{\cdot}7H_2O$	10
(Al_2O_3) nanoparticles	30
Sodium dodecyl sulphate (SDS)	0.5

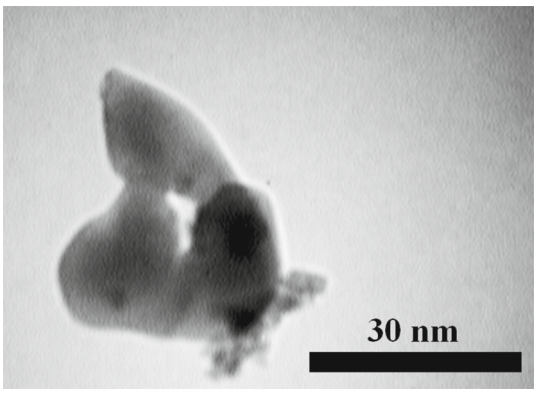

Figure 2. TEM image of alumina nanoparticles used for Ni–Co nanocomposite coatings.

device connected to a computer. A potentiodynamic polarization test was conducted in a solution of 3.5% sodium chloride at ambient temperature and in the potential range of −300 mV to +700 mV *vs*. ocp and at a scan rate of 1 mV s^{-1}. The saturated calomel electrode (SCE) and platinum electrode were used as reference and counter electrodes, respectively. Before the electrochemical test, the samples (the working electrodes) were cleaned in acetone ultrasonically, rinsed in distilled water and dried. Wear tests were performed at room temperature using the pin on disk wear instrument in accordance with the ASTM G99 standard. For this purpose, the vertical force of 10 N with a rotation speed of 5 cm s^{-1} and a movement radius of 1 cm were used. A pin of SAE 52100 steel has been used. Before conducting the wear test, all surfaces were cleaned with acetone and then dried. Weight changes during wear test were measured by using a microbalance with an accuracy of 50 mg. The hardness of the coating was measured using a microhardness device by implementing a force equal to 100 g through a Vickers indenter for 15 s. The indentation size effect was measured by optical microscopy. The samples with different conditions are shown in table 2.

3. Results and discussion

3.1 *Microstructure and chemical composition of the coatings*

SEM micrographs presented in figure 3 show the surface morphologies of functionally graded Ni–Co and Ni–Co–(Al_2O_3) nanocomposite deposits which were produced by gradual change in the duty cycle at constant pulse frequencies of 100, 500 and 1000 Hz. According to figure 3a–f, the grain shapes of all coatings are spherical. Similar morphologies related to Ni–Co coatings were reported [12]. It can be seen that increasing the pulse frequency led to smaller grains, smoother surface and more uniform structures. After completing a pulse, the next pulses are immediately initiated. In this state, supplying the required ions into the electrolyte on the cathode surface might be rather complicated. When the frequency is high, there is no enough time for charging and discharging the double layer at T_{on} and T_{off}, respectively [45], resulting in a high nucleation rate and low growth rate. These conditions lead to compact and finer structures [46].

The cross-section of nickel–cobalt functionally graded coatings with/without alumina nanoparticles is shown in figure 4. All pulse electroplating parameters except for the frequency were the same for all samples. The total thickness of coatings was about 55 μm, so it equals six layers with ∼9 μm. As can be seen in figure 4a and b, coating structure is similar to layers that is deposited on each other. Actually, the layers of coatings are produced by continuous change in duty cycle in each step from 95 to 10%. Due to the similarity of the atomic number of two metallic elements of nickel and cobalt, a scanning electron microscope is not able to identify the gradient coating. But in figure 4b, the alumina nanoparticles can be seen with a gradient distribution in the thickness.

It is necessary to study the distribution of alumina nanoparticles and content of cobalt in the coatings' cross-section to demonstrate the functionally graded structure and variation of chemical composition within the thickness of coatings. Electron microscopy studies and EDS analysis demonstrated that distribution and concentration of alumina nanoparticles and also the content of cobalt in the cross-section increase as a function of thickness. The EDS analysis results of the coatings' cross-section are shown in figure 5. As shown in figure 4a–f, by distancing from the surface of coatings towards the coating/substrate interface, the amount of cobalt increases. In other words, by increasing distance from the coating/substrate interface towards the coating surface, the amount of cobalt has gradually reduced. This indicates the direct impact of the duty cycle on the alloy content in coating. In fact, the process of coating formation is through reducing the duty cycle in the cross-section of coating and thereby reducing it leads to decrease in cobalt content. Co^{2+} concentration is much less than Ni^{2+} in the electrolyte. Thus, increasing the T_{off} at low duty cycle compensates the reduction in Ni^{2+} around the cathode and conditions for ion penetration on the cathode surface are obtained. As a result, the nickel amount in the deposit increases according to others [47,48].

As can be seen in figure 5a–c, the amount of the deposited cobalt increases by increasing the frequency and more clear increment can be observed at a frequency of 1000 Hz. The change in Co content in the coatings by increasing

Table 2. Electroplating conditions of the samples.

Sample	Nanoparticles (g l^{-1})	Frequency (Hz)	i_p (A dm^{-2})	Duty cycle (%)					
				6 st layer	5 st layer	4 st layer	3 st layer	2 st layer	1 st layer
FG-100f	0	100	10	10	25	40	55	70	95
FG-500f	0	500	10	10	25	40	55	70	95
FG-1000f	0	1000	10	10	25	40	55	70	95
FG-NC-100f	30	100	10	10	25	40	55	70	95
FG-NC-500f	30	500	10	10	25	40	55	70	95
FG-NC-1000f	30	1000	10	10	25	40	55	70	95

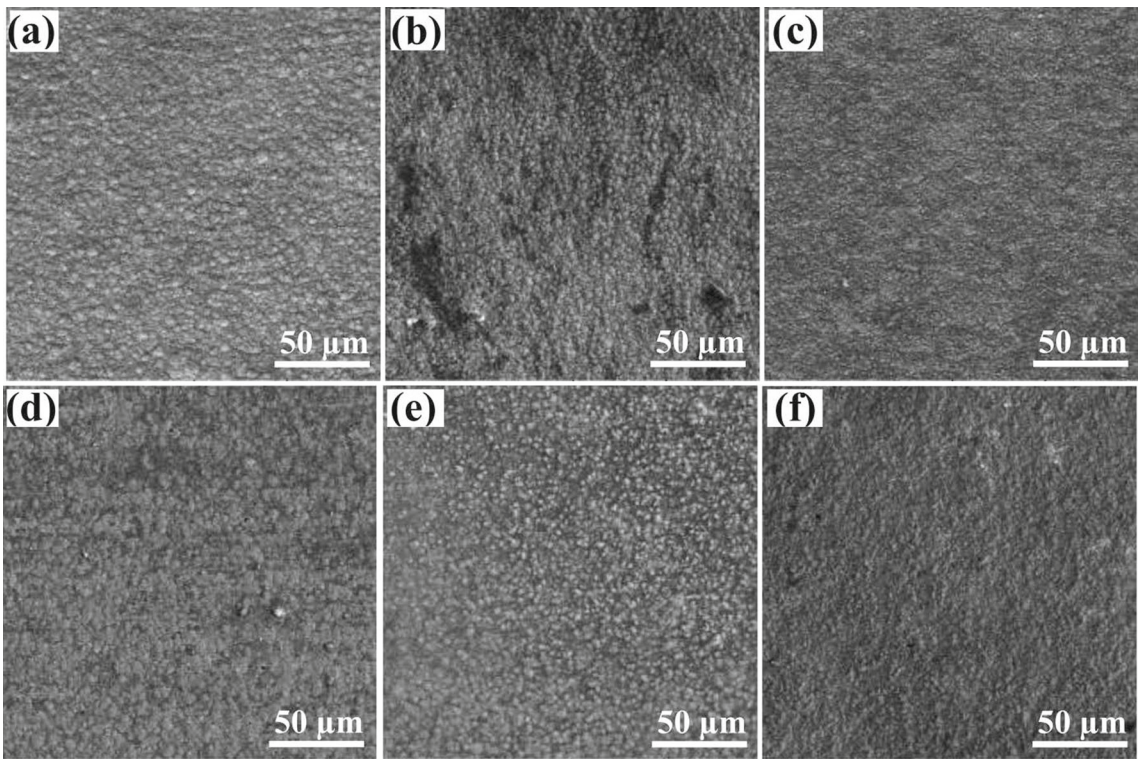

Figure 3. Surface morphology of functionally graded coatings: (**a**) FG-100f, (**b**) FG-500f, (**c**) FG-1000f, (**d**) FG-NC-1000f, (**e**) FG-NC-500f and (**f**) FG-NC-1000f.

the frequency can be related to the anomalous behaviour of coatings. At high frequencies, T_{on} is shorter than at low frequencies, and because of easier deposition of cobalt in the coating, the Co content in the coatings produced at higher pulse frequencies, such as 1000 Hz, is increased.

Figure 6a and b demonstrates the amount of alumina nanoparticles and cross-section of Ni–Co–(Al_2O_3) functionally graded coating. According to figure 6a and c, the alumina nanoparticles have gradually increased by distance from the substrate/coating interface. As can be seen, by increasing the distance from the surface, the amount of alumina nanoparticles is reduced. This is due to the increase in the duty cycle from the coating surface to the coating/substrate interface. By increasing the T_{off} (at a certain frequency) due to reduction in the duty cycle, there is enough time to compensate reduction of nanoparticle content in the double layer. Gradual decrease in duty cycle led to higher nanoparticles in the coating surfaces according to refs. [31,49,50]. It has been shown in other research studies [17,31] that the duty cycle is inversely related to the percentage of nanoparticles in the coating which is confirmed by the obtained results. Unlike duty cycle, frequency has a direct effect on the amount of nanoparticles. Nanoparticles amount slightly increased with increase in the frequency. At high frequencies, low duty cycle and longer off time, better conditions are provided for alumina particles to reach the surface of the substrate and thus, the amount

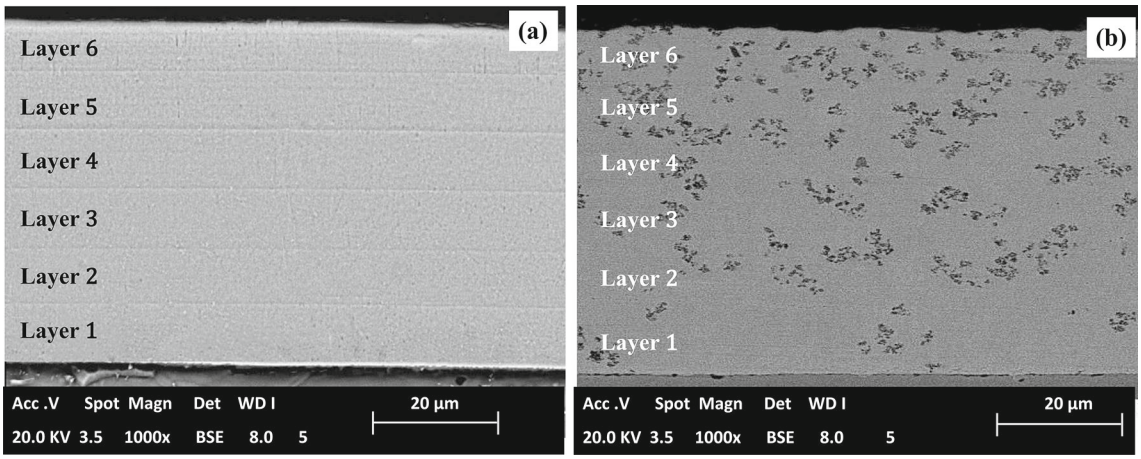

Figure 4. Cross-sectional micrograph of (**a**) FG-100f and (**b**) FG-NC-100f.

of absorbed nanoparticles on the coating surface increases. The current was applied at different frequencies for the same duration, but the cycles of pulses at higher frequencies are more than at lower frequencies. Actually, at higher frequencies, T_{off} is shorter. It makes Ni and Co atoms to capture the nanoparticles. It is possible that some adsorbed alumina particles on the cathode desorbed by hydrodynamic forces in the electrolyte at longer T_{off} of lower frequencies. Therefore, the nanoparticle content had a little increase with rising frequency in agreement to others [51,52]. This is expressible based on the Gugliemi absorption mechanism [53]. In relation to the frequency impact on absorption of nanoparticles, it can be said that during pulsed electrodeposition at lower frequencies, lower over-potential will be created and thus, the required energy for absorption of the neutralized nanoparticles will not be enough as in high frequencies, resulting in a less absorption level of nanoparticles. Also, the frequency has an impact on the microstructure and grain size of the coating. The grain size of the coatings will be reduced by increasing the frequency.

3.2 *Corrosion behaviour*

Figure 7a and b shows the potentiodynamic polarization curves of Ni–Co and Ni–Co–(Al_2O_3) coatings in a solution of 3.5% NaCl at room temperature. As shown in figure 7a and b, it can be seen that all samples have shown an active behaviour in 3.5% sodium chloride solution. The obtained parameters are shown in table 3. The results show that by increasing the frequency from 100 to 1000 Hz, the corrosion current density is raised and corrosion potential is shifted towards negative values. According to the results (table 3), the deposited coatings at lower frequencies (FG-100f and FG-NC-100f samples) had lower i_{corr} in comparison with the fabricated coatings at higher frequencies (FG-1000f and FG-NC-1000f samples). Previous studies [31,47,54] have shown that increasing the frequency leads to the formation of fine-grain coatings. Actually, T_{on} and T_{off} are shorter at higher frequencies. At the beginning of the electrodeposition process, new nuclei formed at T_{on} have no adequate time to grow and quickly T_{off} starts, so it leads to the fine-grain structure. As the grain size of coating decreases (figure 3), the density of grain boundary increases. The coating grain boundaries and other defects act as the preferred locations to corrosion and therefore, increasing the frequency leads to a rise in the corrosion rate. In fact, the grain boundaries form numerous electrochemical microcells with a nickel–cobalt matrix [55]. Another reason for corrosion-resistance reduction by increasing the frequency can be attributed to the chemical composition of Ni–Co electroplated coating (figure 5). In the case of Ni–Co nanocomposite, coatings (figure 7b) can be seen that the corrosion current density reduces through the addition of nanoparticles in comparison with Ni–Co alloy coatings. In fact, the addition of nanoparticles improves the corrosion resistance. The improvement in corrosion resistance of nanocomposite coatings is attributed to the trapped ceramic particles inside the coating [56]. The presence of inactive nanoparticles increases the corrosion resistance in several ways. The nanoparticles act as a barrier against the corrosion. It can be noted that the amount of nanoparticles in the functionally graded coatings is high in the coating surface. Furthermore, this coating is produced in six steps resulting in six layers. This gradient-layered structure of coating acts as a barrier along with nanoparticles and prevent the rapid diffusion of corrosive ions towards the substrate. Moreover, the existence of more complex and longer corrosion paths improves the corrosion resistance due to the presence of nanoparticles [57–59]. The presence of alumina enhances corrosion resistance and E_{corr} is shifted towards more positive values. Actually, the nanoparticles reduce the active surface areas, which is in contact with the corrosive environment [60].

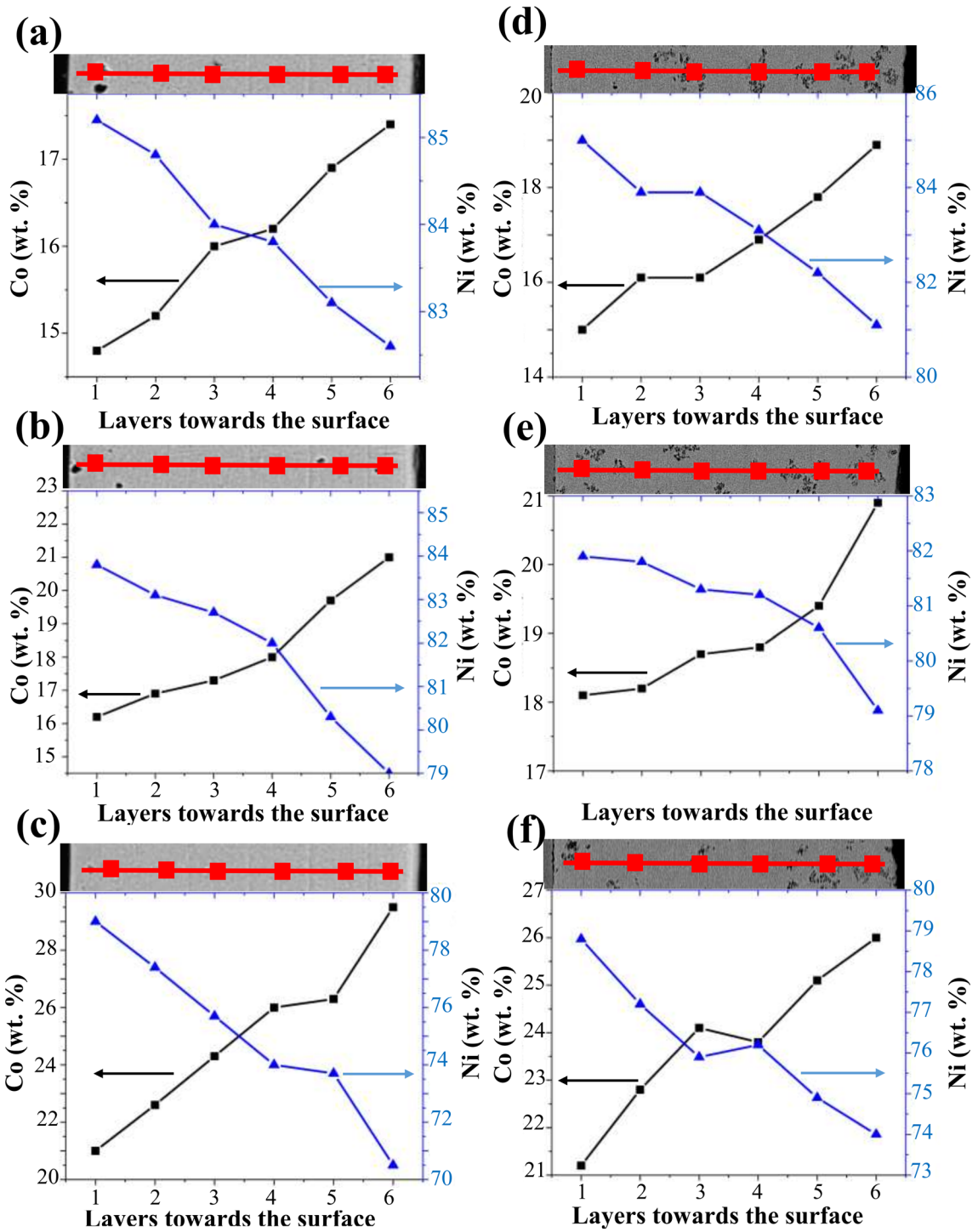

Figure 5. Chemical composition (Co content) of functionally graded coatings: (**a**) FG-100f, (**b**) FG-500f, (**c**) FG-1000f, (**d**) FG-NC-100f, (**e**) FG-NC-500f and (**f**) FG-NC-1000f.

3.3 *Micro-hardness*

The hardness of coatings depends on various factors including the chemical composition, microstructure and strength of the matrix phase. All these factors are influenced by the coating method and its processes. The ceramic nanoparticles are one of the most important factors of hardness improvement in Ni–Co coatings [17,30]. Thus, it can be said that the hardness of coating depends indirectly on the electrodeposition process and is influenced by the bath composition, pH and electroplating current density. The microhardness results of Ni–Co and Ni–Co–alumina coatings

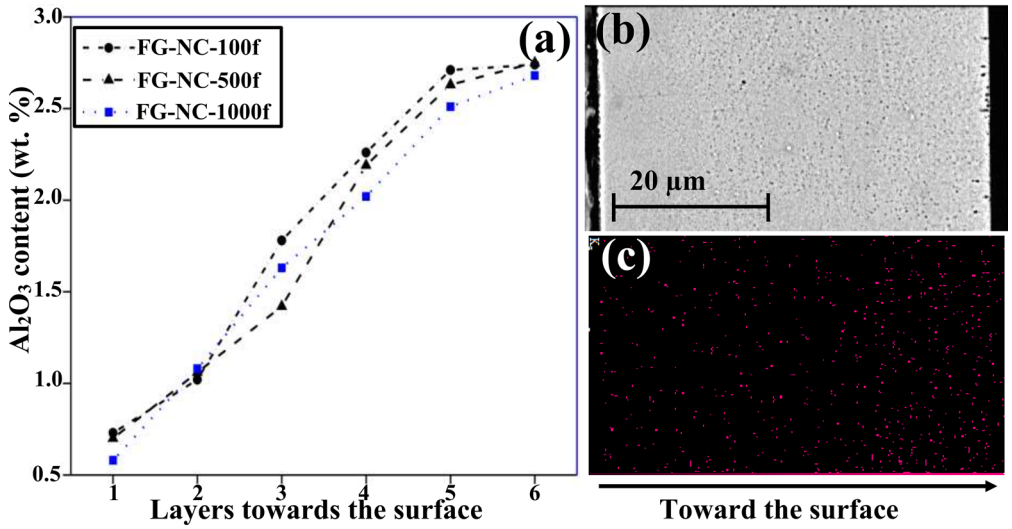

Figure 6. (**a**) Alumina content in functionally graded nanocomposite coatings, (**b**) cross-section and (**c**) EDS map of FG-NC-1000f coating.

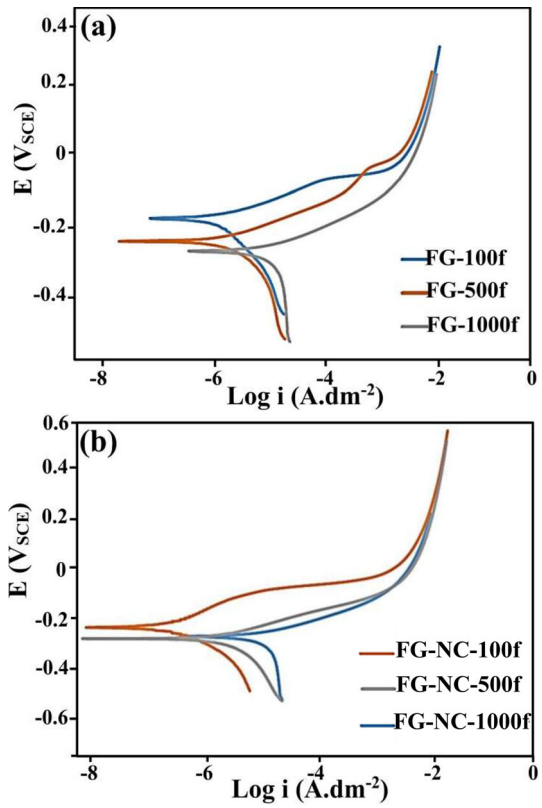

Figure 7. Polarization behaviour of different coated samples in 3.5% sodium chloride solution: (**a**) Ni–Co and (**b**) Ni–Co-(Al_2O_3) functionally graded coatings.

developed at a frequency of 1000 Hz are shown in figure 8. As can be seen, by distancing from the coating/substrate interface, the value of hardness increases (the hardness is equal to 560 Vickers near the coating surface). The hardness of Ni–Co nanocomposite coating is higher than the coating without nanoparticles.

In general, the hardness of nanocomposite material is influenced by two important factors [61]: (1) the amount of strengthener nanoparticles and (2) the hardness of metal matrix. In a specific metal matrix, deposited nanoparticles are the most influential factor on the value of microhardness. The amount and size of nanoparticles have two different hardening mechanisms: (1) the strengthening based on the dispersion hardening and (2) the strengthening based on the particles [18]. Since the strengthener material that is used in this study was at nanoscale, strengthening based on the dispersion hardening is the main microhardness improvement mechanism of the coatings. On the other hand, the hardness of polycrystalline materials is influenced by their microstructure and grain size. And since the deposited coating structure becomes more delicate by changing the electroplating parameters, such as frequency, its hardness will also change. Thereby, reducing the grain size leads to increment in the hardness of the coating. However, in this study, the change of the grain size due to altering electroplating parameters is not enough to shift the value of hardness noticeably. Therefore, it can be concluded that the dominant factor in the determination of coating hardness depends on (Al_2O_3) nanoparticles in the coatings.

3.4 *Wear properties*

The diagram of friction coefficient changes of the Ni–Co and Ni–Co–(Al_2O_3) functionally graded coatings electroplated at different frequencies, under a load of 10 N are shown in figure 9. As can be seen in the figure, a sharp increase in friction coefficient is observed for all samples at the beginning and then it reaches a steady state. Also, it can be seen

Table 3. Corrosion parameters of Ni–Co and Ni–Co–(Al_2O_3) electroplated samples obtained from figure 7.

Sample	FN-100f	FN-500f	FN-1000f	FN-NC-100f	FN-NC-500f	FN-NC-1000f
β_a (mV decade^{-1})	53.8	57.5	58.4	52.5	99.5	62.0
β_c (mV decade^{-1})	165.1	138.5	159.3	162.3	108.6	121.6
E_{corr} (mV *vs.* SCE)	−190.6	−253.8	−268.0	−271.1	−241.5	−291.4
i_{corr} (μA cm^{-2})	1.7	2.0	4.3	1.45	1.5	1.0

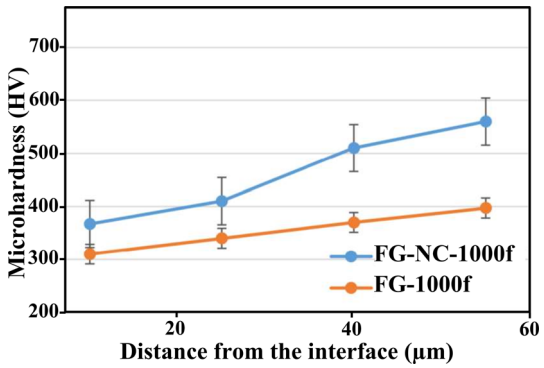

Figure 8. Microhardness values of Ni–Co functionally graded coatings with/without alumina nanoparticles created at the frequency of 1000 Hz.

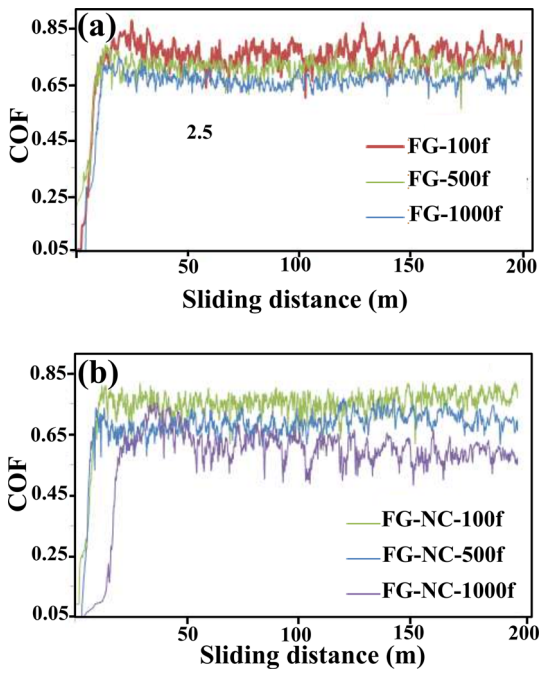

Figure 9. The diagram of friction coefficient *vs.* sliding distance for (**a**) Ni–Co gradient coating and (**b**) nickel–cobalt–alumina gradient coating.

that by increasing the frequency, the coefficient of friction related to the samples with/without nanoparticles is reduced. This can be attributed to two main factors: (1) the chemical composition of the coating and (2) its microstructure. In fact, through increasing the frequency, cobalt content of the coating increases (figure 5) resulting in lower coefficient of friction. This is in agreement with the results of other researchers [11,26]. As the Ni–Co alloys are divided into two categories, Ni-rich and Co-rich, the researches [11] have shown that the friction coefficient of Co-rich Ni–Co alloys is less than that of Ni-rich alloys. Here, the electrodeposited Ni–Co alloys were categorized under the Ni-rich group and thereby as shown in figure 9, no remarkable decrease has been shown compared with pure nickel (friction coefficient of electrodeposited pure Ni is in the range of 0.6–0.8 [11]). The vast reduction in the coefficient of friction in a Co-rich coating in comparison with the Ni-rich coatings probably is due to changes in the crystal structure of the fcc crystalline phase to the hcp phase [11].

Moreover, increasing the frequency leads to a decrease in grain size and also makes a fine structure. This also reduces the coefficient of friction. This has been shown in several studies [44,62]. However, the effect of pulse frequency on the value of friction coefficient in functionally graded coatings is not significant.

Ni–Co coatings containing alumina nanoparticles have a lower friction coefficient (figure 9a) than the coatings without nanoparticles (figure 9b). In fact, Ni–Co–(Al_2O_3) coatings have a higher hardness compared with the coatings without alumina nanoparticles and this leads to a reduction in the contact area between the involved components. Also, the presence of nanoparticles can ease the slide mechanism resulting in a decrease in the friction coefficient of these coatings compared with the no nanoparticle containing coatings [63]. But in general, the coefficient of friction is influenced by two principal factors including Co content of the coating and the amount of the nanoparticles in the coatings. In other words, these two factors can improve the frictional properties of nickel–cobalt coatings.

Figure 10 shows the worn surface of Ni–Co and Ni–Co–(Al_2O_3) coatings at different frequencies. The width of wear path of the Ni–Co–(Al_2O_3) coating is smaller than the Ni–Co coatings. With regards to this, it can be said that the Ni–Co–(Al_2O_3) composite coatings have better wear resistance than Ni–Co coatings. Scuffing effects along with plastic deformation and worn debris in the worn path of the coatings can be observed from figure 10a–c. Severe adhesive and abrasive wear with a greater width of wear path were observed for the FG-100f coating. According to these and SEM images, it can

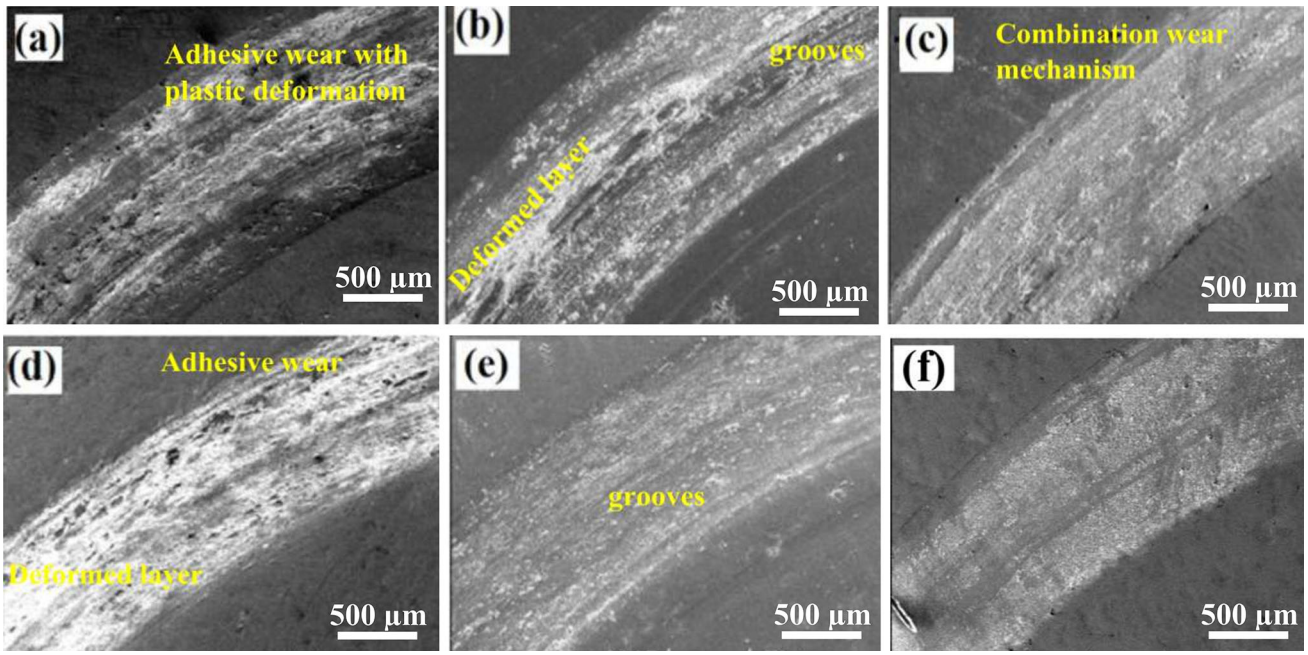

Figure 10. SEM images of worn surfaces after wear test for (**a**) FG-100f, (**b**) FG-500f, (**c**) Fg-1000f, (**d**) FG-NC-100f, (**e**) FG-NC-500f and (**f**) FG-NC-1000f.

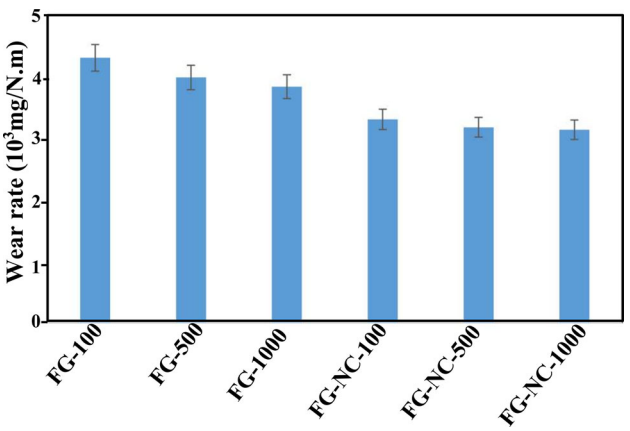

Figure 11. Wear rate values Ni–Co and Ni–Co–(Al_2O_3) functionally graded coatings.

be concluded that the wear mechanism is a combination of adhesive and abrasive wear modes. The amount of scuffing effects and plastic deformation of Ni–Co–(Al_2O_3) functionally graded coatings are partly lower (figures 8f and 10d). Also, due to the conduction of the wear test, some fine abrasive grooves appear on the worn surfaces. It can be concluded that the dominant mechanism in the Ni–Co–(Al_2O_3) composite coatings is the abrasive wear with minor adhesive wear. The existence of ceramic nanoparticles has helped Ni–Co coatings in terms of wear properties' improvement. This topic has been shown in various studies [30,61].

The wear rate values of Ni–Co and Ni–Co–(Al_2O_3) functionally graded coatings developed at different frequencies are shown in figure 11. As can be seen in this figure, in general, the wear rate values of samples with Ni–Co coatings are higher than those of Ni–Co–Al_2O_3 coatings. This behaviour is in agreement with what was previously observed in other works that grain refinement could improve wear resistance [64,65]. It was observed that the wear resistance is independent of the grain size and it depends on the coating strength [66]. However, the loss of wear resistance has been reported in some ultrafine grain and nanometric structures [66]. The wear rate in a pin on disk test is directly related to parameters, such as (1) the applied load, (2) wear distance x and (3) hardness in reverse H [67]:

$$q = Wx/H. \tag{1}$$

According to this equation, wear rate is inversely related to the hardness. By comparing the wear rates of coatings (figure 11) with results of hardness (figure 8) which were conducted on the nickel–cobalt electroplated samples at a frequency of 1000 Hz, it is concluded that the value of hardness increases across the entire thickness of the coating by the addition of nanoparticles. The wear rates result also shows that the rate of wear is inversely correlated with a hardness of the samples. In general, in the coatings, the hardness increases by increasing the frequency [63] and in the Ni-rich nickel–cobalt coating, the value of hardness increases by increasing the cobalt content [11] and thereby it can be concluded that the frequency or cobalt content have positive effect on wear resistance.

4. Conclusions

In this study, Ni–Co and Ni–Co–(Al_2O_3) gradient coatings using pulsed electroplating at frequencies of 100, 500 and 1000 Hz by changing the duty cycle continuously, were developed on the low-carbon steel substrate. The results of this study are summarized as follows:

(1) By reducing the duty cycle from coating/substrate interface towards the surface of the coating, the amount of nanoparticles increases and alloy cobalt content decreases. Frequency does not have much impact on the alloy content of the coatings.
(2) The amount of corrosion steps up with the increase in the value of frequency. The nanoparticle has a positive impact on the corrosion resistance of the nickel–cobalt coating.
(3) The hardness of gradient coatings gradually increases by moving from the interface towards the surface. The existence of nanoparticles leads to increase in hardness.
(4) The studies on the friction coefficient showed that the surface friction coefficient reduced by increasing the frequency of nickel–cobalt coatings with/without alumina nanoparticles.

References

[1] Narayanan T, Shaijumon M, Ajayan P and Anantharaman M 2010 *Nanoscale Res. Lett.* **5** 164
[2] Shi L, Sun C, Gao P, Zhou F and Liu W 2006 *Appl. Surf. Sci.* **252** 3591
[3] Chi B, Li J, Yang X, Gong Y and Wang N 2005 *Int. J. Hydrogen Energy* **30** 29
[4] Oriňáková R, Turoňová A, Kladeková D, Gálová M and Smith R M 2006 *J. Appl. Electrochem.* **36** 957
[5] Kim D, Park D-Y, Yoo B, Sumodjo P and Myung N 2003 *Electrochim. Acta* **48** 819
[6] Li Y, Tao Y, Ke D, Ma Y and Han S 2015 *Appl. Surf. Sci.* **357** 1714
[7] Tian L, Xu J and Qiang C 2011 *Appl. Surf. Sci.* **257** 4689
[8] Farzaneh M, Zamanzad-Ghavidel M, Raeissi K, Golozar M, Saatchi A and Kabi S 2011 *Appl. Surf. Sci.* **257** 5919
[9] El-Feky H, Negem M, Roy S, Helal N and Baraka A 2013 *Sci. China Chem.* **56** 1446
[10] Li Y, Jiang H, Wang D and Ge H 2008 *Surf. Coat. Technol.* **202** 4952
[11] Wang L, Gao Y, Xue Q, Liu H and Xu T 2005 *Appl. Surf. Sci.* **242** 326
[12] Zamani M, Amadeh A and Baghal S L 2016 *Trans. Nonferrous Met. Soc. China* **26** 484
[13] Dai P, Zhong Y and Zhou X 2011 *Surf. Eng.* **27** 71
[14] Tian B and Cheng Y 2007 *Electrochim. Acta* **53** 511
[15] Yang Y and Cheng Y 2011 *Surf. Coat. Technol.* **205** 3198
[16] Vijayakumar J, Mohan S, Kumar S A, Suseendiran S and Pavithra S 2013 *Int. J. Hydrogen Energy* **38** 10208
[17] Yang Y and Cheng Y 2013 *Surf. Coat. Technol.* **216** 282
[18] Chen L, Wang L, Zeng Z and Zhang J 2006 *Mater. Sci. Eng. A* **434** 319
[19] Chen W, Tu J, Gan H, Xu Z, Wang Q, Lee J *et al* 2002 *Surf. Coat. Technol.* **160** 68
[20] Wang Y, Tay S L, Wei S, Xiong C, Gao W, Shakoor R *et al* 2015 *J. Alloys Compd.* **649** 222
[21] Harsha S, Dwivedi D and Agrawal A 2007 *Surf. Coat. Technol.* **201** 5766
[22] Vazquez-Arenas J, Treeratanaphitak T and Pritzker M 2012 *Electrochim. Acta* **62** 63
[23] Vazquez-Arenas J, Altamirano-Garcia L, Treeratanaphitak T, Pritzker M, Luna-Sánchez R and Cabrera-Sierra R 2012 *Electrochim. Acta* **65** 234
[24] Tury B, Radnóczi G, Radnóczi G and Varsányi M 2007 *Surf. Coat. Technol.* **202** 331
[25] Chang L, An M and Shi S 2005 *Mater. Chem. Phys.* **94** 125
[26] Wang L, Gao Y, Xue Q, Liu H and Xu T 2005 *J. Phys. D: Appl. Phys.* **38** 1318
[27] Bostani B, Parvini Ahmadi N and Yazdani S 2016 *Surf. Eng.* **32** 495
[28] Orlovskaja L, Periene N, Kurtinaitiene M and Bikulčius G 1998 *Surf. Coat. Technol.* **105** 8
[29] Hou K, Ger M, Wang L and Ke S 2002 *Wear* **253** 994
[30] Baghal S L, Sohi M H and Amadeh A 2012 *Surf. Coat. Technol.* **206** 4032
[31] Lajevardi S, Shahrabi T, Szpunar J, Rouhaghdam A S and Sanjabi S 2013 *Surf. Coat. Technol.* **232** 851
[32] García-Lecina E, García-Urrutia I, Díez J, Salvo M, Smeacetto F, Gautier G *et al* 2009 *Electrochim. Acta* **54** 2556
[33] Dong Y, Lin P and Wang H 2006 *Surf. Coat. Technol.* **200** 3633
[34] Wang H, Yao S and Matsumura S 2004 *J. Mater. Process. Technol.* **145** 299
[35] Torabinejad V, Aliofkhazraei M, Rouhaghdam A S and Allahyarzadeh M 2017 *Wear* **380** 115
[36] Allahyarzadeh M, Aliofkhazraei M, Rouhaghdam A S and Torabinejad V 2017 *J. Alloys Compd.* **705** 788
[37] Majidi H, Aliofkhazraei M, Karimzadeh A and Rouhaghdam A S 2017 *Can. Metall. Q* **56** 179
[38] Torabinejad V, Rouhaghdam A S, Aliofkhazraei M and Allahyarzadeh M 2016 *J. Alloys Compd.* **657** 526
[39] Allahyarzadeh M, Aliofkhazraei M, Rouhaghdam A S and Torabinejad V 2017 *Surf. Eng.* **33** 327
[40] Baghal S L, Amadeh A, Sohi M H and Hadavi S 2013 *Mater. Sci. Eng. A* **559** 583
[41] Ma E 2003 *Scr. Mater.* **49** 663
[42] Qin L, Lian J and Jiang Q 2010 *J. Alloys Compd.* **504** S439
[43] Cavaliere P 2008 *Comput. Mater. Sci.* **41** 440
[44] Allahyarzadeh M, Aliofkhazraei M, Rouhaghdam A S and Torabinejad V 2016 *J. Alloys Compd.* **666** 217
[45] Chang L, Liu W, Duan X and Xu J 2012 *Surf. Eng.* **28** 725
[46] Hammami O, Dhouibi L, Berçot P and Rezrazi E M 2014 *J. Appl. Electrochem.* **44** 115
[47] Ghazanlou S I, Farhood A, Hosouli S, Ahmadiyeh S and Rasooli A 2017 *J. Mater. Sci.: Mater. Electron.* **28** 1
[48] Boonyongmaneerat Y, Saengkiettiyut K, Saenapitak S and Sangsuk S 2014 *J. Mater. Eng. Perform.* **23** 302
[49] Lajevardi S, Shahrabi T and Szpunar J 2013 *Appl. Surf. Sci.* **279** 180
[50] Bahrololoom M and Sani R 2005 *Surf. Coat. Technol.* **192** 154

[51] Thiemig D, Lange R and Bund A 2007 *Electrochim. Acta* **52** 7362
[52] Chen L, Wang L, Zeng Z and Xu T 2006 *Surf. Coat. Technol.* **201** 599
[53] Guglielmi N 1972 *J. Electrochem. Soc.* **119** 1009
[54] Ghazanlou S I, Ahmadiyeh S and Yavari R 2017 *Surf. Eng.* **33** 337
[55] Goldasteh H and Rastegari S 2014 *Surf. Coat. Technol.* **259** 393
[56] Feng Q, Li T, Teng H, Zhang X, Zhang Y, Liu C *et al* 2008 *Surf. Coat. Technol.* **202** 4137
[57] Gupta R, Das A, Nagahanumaiah and Henal S 2016 *Mater. Manuf. Process.* **31** 42
[58] Rezaeiolum A, Aliofkhazraei M, Karimzadeh A, Rouhaghdam A and Miresmaeili R 2017 *Surf. Eng.* **34** 1
[59] Soleimani R, Mahboubi F, Kazemi M and Arman S 2015 *Surf. Eng.* **31** 714
[60] Sajjadnejad M, Omidvar H, Javanbakht M, Pooladi R and Mozafari A 2014 *Trans. IMF* **92** 227
[61] Sharma G, Yadava R and Sharma V 2006 *Bull. Mater. Sci.* **29** 491
[62] Torabinejad V, Aliofkhazraei M, Rouhaghdam A S and Allahyarzadeh M 2016 *J. Mater. Eng. Perform.* **25** 5494
[63] Torabinejad V, Aliofkhazraei M, Rouhaghdam A S and Allahyarzadeh M 2017 *Tribol. Trans.* **60** 923
[64] Mishra R, Basu B and Balasubramaniam R 2004 *Mater. Sci. Eng. A* **373** 370
[65] Jeong D, Gonzalez F, Palumbo G, Aust K and Erb U 2001 *Scr. Mater.* **44** 493
[66] Hanlon T, Chokshi A, Manoharan M and Suresh S 2005 *Int. J. Fatigue* **27** 1159
[67] Ramezanalizadeh H, Emamy M and Shokouhimehr M 2016 *Tribol. Trans.* **59** 219